

EFFICIENT SUPER-RESOLUTION TWO-DIMENSIONAL HARMONIC RETRIEVAL VIA ENHANCED LOW-RANK STRUCTURED COVARIANCE RECONSTRUCTION

Yue Wang* Yu Zhang†* Zhi Tian* Geert Leus‡ Gong Zhang†

*Department of ECE, George Mason University, Fairfax, VA, USA

†College of EIE, Nanjing University of Aeronautics and Astronautics, Nanjing, China

‡Faculty of EEMCS, Delft University of Technology, Delft, The Netherlands

ABSTRACT

This paper develops an enhanced low-rank structured covariance reconstruction (LRSCR) method based on the decoupled atomic norm minimization (D-ANM), for super-resolution two-dimensional (2D) harmonic retrieval with multiple measurement vectors. This LRSCR-D-ANM approach exploits a potential structure hidden in the covariance by transferring the basic LRSCR to an efficient D-ANM formulation, which permits a sparse representation over a matrix-form atom set with decoupled 1D frequency components. The new LRSCR-D-ANM method builds upon the existence of a generalized Vandermonde decomposition of its solution, which otherwise cannot be guaranteed by the basic LRSCR unless a very conservative condition holds. Further, a low-complexity solution of the LRSCR-D-ANM is provided for fast implementation with negligible performance loss. Simulation results verify the advantages of the proposed LRSCR-D-ANM over the basic LRSCR, in terms of the wider applicability and the lower complexity.

Index Terms— Super-resolution, 2D harmonic retrieval, MMV, LRSCR, D-ANM.

1. INTRODUCTION

In harmonic retrieval with multiple measurement vectors (MMV), to fix the computational complexity of the atomic norm minimization (ANM) methods [1, 2], a super-resolution technique called the low-rank structured covariance reconstruction (LRSCR) was proposed based on the covariance matrix whose size does not increase with the number of MMV [3–5]. The LRSCR jointly utilizes two important properties of the covariance matrix, i.e., the low-rankness and the Toeplitz structure, which have been treated separately in [6, 7].

For two-dimensional (2D) scenarios, the LRSCR originally developed in 1D cases [3, 4], can be straightforwardly extended to its 2D version [8]. However, such a simple extension of the basic LRSCR leads to a very conservative condition in terms of the maximum number of detectable 2D harmonics with MMV. When the number of 2D harmonics goes beyond such an upper-bound, an extra checking mechanism has to be adopted to check the existence of the solution [9, 10]. This checking scheme was however originally designed for the single measurement vector (SMV) case, and intuitively could be skipped thanks to the supplementary measurements

This work was supported in part by the US National Science Foundation (NSF) grants #1527396 and #1547364, and the National Science Foundation of China (NSFC) grants #61871218, #61471191, #61801211 and #61501228. This work was partly carried out in the frame of the ASPIRE project (project 14926 within the OTP program of NWO-TTW).

collected from MMV beyond SMV. Moreover, although the complexity of the LRSCR is independent of the number of MMV, its implementation in 2D scenarios still causes a tremendously high computational cost in order to implement the two-level Toeplitz structure of the large-size covariance.

To overcome the aforementioned problems under the LRSCR framework, this paper proposes an efficient super-resolution technique for 2D harmonic retrieval with MMV. It exploits the structure of a kernel matrix of reduced size, which is hidden in the large-size two-level Toeplitz structured covariance. This structure is effectively captured, when the basic LRSCR based on the covariance matrix is transformed as a decoupled atomic norm minimization (D-ANM) formulation (termed LRSCR-D-ANM) based on this kernel matrix. It is the utilization of the sparse structure of the kernel matrix through the D-ANM that essentially boosts the upper-bound on the number of detectable 2D harmonics beyond that of the basic LRSCR. Further, for fast implementation, we also provide an alternative low-complexity version of the LRSCR-D-ANM, by removing the largest-size constraint from its semidefinite programming (SDP) formulation with negligible performance degradation. This reflects a desired tradeoff between the estimation accuracy and the computational complexity, which can be achieved by the LRSCR-D-ANM. Simulation results indicate that the proposed LRSCR-D-ANM solutions outperform the basic LRSCR by accurately retrieving more detectable 2D harmonics in less runtime.

Notations: a , \mathbf{a} , \mathbf{A} , and \mathcal{A} denote a scalar, a vector, a matrix, and an atom set, respectively. $(\cdot)^T$, $(\cdot)^*$, and $(\cdot)^H$ are the transpose, conjugate, and conjugate transpose of a vector or matrix, respectively. $\|\mathbf{a}\|_2$ is the ℓ_2 -norm of \mathbf{a} . $\text{diag}(\mathbf{a})$ generates a diagonal matrix with the diagonal elements constructed from \mathbf{a} . $\|\mathbf{A}\|_F$, $\|\mathbf{A}\|_{\mathcal{A}}$, $\text{Tr}(\mathbf{A})$, and $\text{Rank}(\mathbf{A})$ are the Frobenius norm, the atomic norm, the trace, and the rank of \mathbf{A} , respectively. \mathbf{I} is an identity matrix. \mathbf{T} and \mathbf{T}' represent Hermitian Toeplitz and Toeplitz matrices, respectively. $\mathcal{S}(\mathbf{A})$ indicates a unique mapping from \mathbf{A} to a two-level Toeplitz matrix \mathbf{T}_{2D} . $\mathbb{E}\{\cdot\}$ represents expectation. \otimes and \odot denote the Kronecker product and the Khatri-Rao product operations, respectively.

2. SIGNAL MODEL

Consider an MMV model with L snapshots where the signal of interest $\mathbf{x}(t) \in \mathbb{C}^{NM}$ is a linear mixture of K 2D sinusoidal components contaminated by additive Gaussian noise $\mathbf{n}(t) \sim \mathcal{CN}(\mathbf{0}, \sigma^2 \mathbf{I})$ in the form of

$$\begin{aligned} \mathbf{x}(t) &= \sum_{i=1}^K s_i(t) \mathbf{a}_N(f_{1,i}) \otimes \mathbf{a}_M(f_{2,i}) + \mathbf{n}(t) \\ &= (\mathbf{A}_N(\mathbf{f}_1) \odot \mathbf{A}_M(\mathbf{f}_2)) \mathbf{s}(t) + \mathbf{n}(t), \quad t = 1, \dots, L, \end{aligned} \quad (1)$$

where $\mathbf{s}(t)=[s_1(t), \dots, s_K(t)]^T$, $\mathbf{f}_1=[f_{1,1}, \dots, f_{1,K}]$ and $\mathbf{f}_2=[f_{2,1}, \dots, f_{2,K}]$ denote the complex amplitudes and the digital frequencies along two orthogonal dimensions of the K sources with $\{f_{1,i}, f_{2,i}\} \in [-0.5, 0.5]^2$, and $\mathbf{A}_N(\mathbf{f}_1)=[\mathbf{a}_N(f_{1,1}), \dots, \mathbf{a}_N(f_{1,K})]$ and $\mathbf{A}_M(\mathbf{f}_2)=[\mathbf{a}_M(f_{2,1}), \dots, \mathbf{a}_M(f_{2,K})]$ are the manifold matrices with their columns $\mathbf{a}_N(f_{1,i})$ and $\mathbf{a}_M(f_{2,i})$ exhibiting the Vandermonde structures of size N and M respectively [11–13],

$$\begin{aligned} \mathbf{a}_N(f_{1,i}) &= [1, \exp(j2\pi f_{1,i}), \dots, \exp(j2\pi(N-1)f_{1,i})]^T, \\ \mathbf{a}_M(f_{2,i}) &= [1, \exp(j2\pi f_{2,i}), \dots, \exp(j2\pi(M-1)f_{2,i})]^T. \end{aligned} \quad (2)$$

In many applications, $\mathbf{x}(t)$ in (1) is not observed directly, but over a linear compressive measurement matrix $\mathbf{J} \in \mathbb{C}^{M' \times NM}$ with $M' \leq NM$ as

$$\mathbf{y}(t) = \mathbf{J}\mathbf{x}(t) = \mathbf{J}(\mathbf{A}_N(\mathbf{f}_1) \odot \mathbf{A}_M(\mathbf{f}_2)) \mathbf{s}(t) + \mathbf{J}\mathbf{n}(t). \quad (3)$$

Then, the covariance matrix of $\mathbf{y}(t)$ can be expressed as

$$\mathbf{R}_y = \mathbb{E}\{\mathbf{y}(t)\mathbf{y}(t)^H\} = \mathbf{J}\mathbf{R}_x\mathbf{J}^H + \sigma^2\mathbf{J}\mathbf{J}^H, \quad (4)$$

where \mathbf{R}_x is the covariance matrix of $\mathbf{x}(t)$ given by

$$\mathbf{R}_x = (\mathbf{A}_N(\mathbf{f}_1) \odot \mathbf{A}_M(\mathbf{f}_2))\mathbf{R}_s(\mathbf{A}_N(\mathbf{f}_1) \odot \mathbf{A}_M(\mathbf{f}_2))^H, \quad (5)$$

where $\mathbf{R}_s = \text{diag}([r_1, \dots, r_K]^T) = \text{diag}(\mathbf{r}) \succeq 0$ is a positive semidefinite (PSD) diagonal matrix under the assumption that $s_i(t)$ in $\mathbf{s}(t)$ is uncorrelated with each other. Given a collection of sufficient MMV, the estimation of \mathbf{R}_y in (4) can be approximately calculated as its sample covariance $\hat{\mathbf{R}}_y = \frac{1}{L} \sum_{t=1}^L \mathbf{y}(t)\mathbf{y}(t)^H$. Then, the goal of the covariance-based 2D harmonic retrieval is to recover the unknown harmonics \mathbf{f}_1 and \mathbf{f}_2 from $\hat{\mathbf{R}}_y$.

3. ENHANCED LOW-RANK STRUCTURED COVARIANCE RECONSTRUCTION

In this section, we present a super-resolution 2D harmonic retrieval with MMV under the LRSCR framework. Specifically, we enhance the basic LRSCR by reformulating it to an improved version named LRSCR-D-ANM. It better captures the strong structure hidden in the covariance matrix via D-ANM, which otherwise cannot be explicitly exploited by the basic LRSCR formulation. In doing so, we start by rewriting (5) as

$$\mathbf{R}_x = \sum_{i=1}^K r_i (\mathbf{a}_N(f_{1,i}) \otimes \mathbf{a}_M(f_{2,i})) (\mathbf{a}_N(f_{1,i}) \otimes \mathbf{a}_M(f_{2,i}))^H \quad (6a)$$

$$= \sum_{i=1}^K r_i (\mathbf{a}_N(f_{1,i}) \mathbf{a}_N^H(f_{1,i})) \otimes (\mathbf{a}_M(f_{2,i}) \mathbf{a}_M^H(f_{2,i})). \quad (6b)$$

3.1. Basic LRSCR

On the one hand, according to (6a), \mathbf{R}_x is obviously a Hermitian matrix with a two-level Toeplitz structure that can be represented as

$$\mathbf{R}_x = \mathbf{T}_{2D}(\mathbf{u}_{R_x}, \mathbf{v}_{R_x}), \quad (7)$$

where $\mathbf{u}_{R_x} = \sum_{i=1}^K r_i \mathbf{a}_N(f_{1,i}) \otimes \mathbf{a}_M(f_{2,i}) \in \mathbb{C}^{NM}$ and $\mathbf{v}_{R_x} = \sum_{i=1}^K r_i \mathbf{a}_{N_1}(f_{1,i}) \otimes \mathbf{a}_{M_1}^*(f_{2,i}) \in \mathbb{C}^{(N-1)(M-1)}$ with $\mathbf{a}_{N_1}(f_{1,i})$ and $\mathbf{a}_{M_1}(f_{2,i})$ being the last $N-1$ and $M-1$ rows of $\mathbf{a}_N(f_{1,i})$ and $\mathbf{a}_M(f_{2,i})$ in (2), respectively. Accordingly, \mathbf{R}_x is not only a low-rank matrix with rank equal to K , but it is also equipped with a two-level Toeplitz structure.

Then, following the low-rank covariance matrix recovery theory [6], the covariance matrix in (7) can be recovered by solving a relaxed problem of the nonconvex rank minimization via a trace minimization, which leads to the basic LRSCR for 2D frequency retrieval [8]

$$\begin{aligned} \{\tilde{\mathbf{u}}_{R_x}, \tilde{\mathbf{v}}_{R_x}\} &= \arg \min_{\mathbf{u}_{R_x}, \mathbf{v}_{R_x}} \text{Tr}(\mathbf{T}_{2D}(\mathbf{u}_{R_x}, \mathbf{v}_{R_x})) \\ \text{s.t.} \quad &\left\| \hat{\mathbf{R}}_y - \mathbf{J}\mathbf{T}_{2D}(\mathbf{u}_{R_x}, \mathbf{v}_{R_x})\mathbf{J}^H \right\|_F^2 \leq \beta, \\ &\mathbf{T}_{2D}(\mathbf{u}_{R_x}, \mathbf{v}_{R_x}) \succeq 0, \end{aligned} \quad (8)$$

where β is a user-specified parameter based on a certain error tolerance, which can be set according to σ^2 . When the noise statistics are unavailable or hard to obtain in practice, β can be determined via the covariance matrix sparse representation method [14], or by using the covariance matrix fitting criterion [15, 16].

Remark 1: Noticeably, the recovered $\mathbf{T}_{2D}(\tilde{\mathbf{u}}_{R_x}, \tilde{\mathbf{v}}_{R_x})$ from (8) cannot be guaranteed to be the exact solution of \mathbf{R}_x as indicated by (7). This is because the existence of the generalized Vandermonde decomposition of $\mathbf{T}_{2D}(\tilde{\mathbf{u}}_{R_x}, \tilde{\mathbf{v}}_{R_x})$ cannot be guaranteed unless $\text{Rank}(\mathbf{T}_{2D}(\tilde{\mathbf{u}}_{R_x}, \tilde{\mathbf{v}}_{R_x})) \leq \min\{N, M\} - 1$ holds, according to the generalized Vandermonde decomposition lemma [10]. However, given the more measurements available from MMV compared to SMV, this condition seems too conservative for the MMV case as it is solely based on the SMV case [10].

3.2. LRSCR-D-ANM

On the other hand, based on (6b), \mathbf{R}_x can be rewritten as

$$\begin{aligned} \mathbf{R}_x &= \mathcal{S}(\mathbf{K}) \\ &= \begin{bmatrix} \mathbf{T}'(\mathbf{u}^0) & \mathbf{T}'(\mathbf{u}^{-1}) & \dots & \mathbf{T}'(\mathbf{u}^{-(N-1)}) \\ \mathbf{T}'(\mathbf{u}^1) & \mathbf{T}'(\mathbf{u}^0) & \dots & \mathbf{T}'(\mathbf{u}^{-(N-2)}) \\ \vdots & \vdots & \ddots & \vdots \\ \mathbf{T}'(\mathbf{u}^{N-1}) & \mathbf{T}'(\mathbf{u}^{N-2}) & \dots & \mathbf{T}'(\mathbf{u}^0) \end{bmatrix}, \end{aligned} \quad (9)$$

where $\mathbf{T}'(\mathbf{u}^l) \in \mathbb{C}^{M \times M}$, $l = -(N-1), \dots, 0, \dots, N-1$ is a Toeplitz matrix given by

$$\mathbf{T}'(\mathbf{u}^l) = \begin{bmatrix} u_0^l & u_{-1}^l & \dots & u_{-(M-1)}^l \\ u_1^l & u_0^l & \dots & u_{-(M-2)}^l \\ \vdots & \vdots & \ddots & \vdots \\ u_{M-1}^l & u_{M-2}^l & \dots & u_0^l \end{bmatrix}, \quad (10)$$

with $u_m^l = \sum_{i=1}^K r_i e^{j2\pi(lf_{1,i} - mf_{2,i})}$, $m = -(M-1), \dots, 0, \dots, M-1$ and $\mathbf{u}^l = [u_{-(M-1)}^l, \dots, u_{-1}^l, u_0^l, u_1^l, \dots, u_{M-1}^l]^T \in \mathbb{C}^{2M-1}$ collecting the unique elements of $\mathbf{T}'(\mathbf{u}^l)$.

We define \mathbf{K} as the kernel matrix of the covariance matrix $\mathbf{R}_x = \mathcal{S}(\mathbf{K})$ in (9) as

$$\mathbf{K} = [\mathbf{u}^{-(N-1)}, \dots, \mathbf{u}^{-1}, \mathbf{u}^0, \mathbf{u}^1, \dots, \mathbf{u}^{N-1}] \in \mathbb{C}^{(2M-1) \times (2N-1)}. \quad (11)$$

Now, we study how to exploit the potential structure of \mathbf{K} , in order to enforce the existence of the generalized Vandermonde decomposition of the estimation of \mathbf{R}_x which however cannot be guaranteed by the solution from (8). From (6), (9) and (10), it can be shown that the columns of \mathbf{K} in (11) can be equivalently expressed by

$$\mathbf{u}^l = \sum_{i=1}^K r_i e^{j2\pi l f_{1,i}} \mathbf{a}'_M(f_{2,i}), \quad l = -(N-1), \dots, 0, \dots, N-1, \quad (12)$$

where $\mathbf{a}'_M(f_{2,i}) \in \mathbb{C}^{2M-1}$ is defined as

$$\begin{aligned} \mathbf{a}'_M(f_{2,i}) &= [e^{-j2\pi(M-1)f_{2,i}}, \dots, e^{-j2\pi f_{2,i}}, 1, e^{j2\pi f_{2,i}}, \dots, e^{j2\pi(M-1)f_{2,i}}]^T. \end{aligned} \quad (13)$$

Then, given (12), \mathbf{K} defined in (11) can be rewritten as

$$\mathbf{K} = \sum_{i=1}^K r_i \mathbf{a}'_M(f_{2,i}) \mathbf{a}'_N(f_{1,i})^T = \mathbf{A}'_M(\mathbf{f}_2) \text{diag}(\mathbf{r}) \mathbf{A}'_N(\mathbf{f}_1)^T, \quad (14)$$

where $\mathbf{a}'_N(f_{1,i}) \in \mathbb{C}^{2N-1}$ is defined similarly to (13) by replacing M and $f_{2,i}$ in (13) with N and $f_{1,i}$, and $\mathbf{A}'_M(\mathbf{f}_2)$ and $\mathbf{A}'_N(\mathbf{f}_1)$ are formed with $\mathbf{a}'_M(f_{2,i})$ and $\mathbf{a}'_N(f_{1,i})$ being their columns, respectively. Connecting (6b) and (14), we have the following proposition.

Proposition 1: If \mathbf{K} has a decomposition in the form of (14) and is a low-rank matrix satisfying $K \leq 2 \min\{N, M\} - 2$, then $\mathcal{S}(\mathbf{K})$ has the generalized Vandermonde decomposition in the form of (6b) and is a low-rank matrix with the same rank of \mathbf{K} , i.e., $\text{Rank}(\mathcal{S}(\mathbf{K})) = \text{Rank}(\mathbf{K}) = K$.

Proof: Going through (9) to (14), we have: if $\mathcal{S}(\mathbf{K})$ has the generalized Vandermonde decomposition in the form of (6b) and is a low-rank matrix satisfying $K \leq 2 \min\{N, M\} - 2$, then \mathbf{K} has the decomposition in the form of (14) and is a low-rank matrix with the same rank of $\mathcal{S}(\mathbf{K})$, i.e., $\text{Rank}(\mathbf{K}) = \text{Rank}(\mathcal{S}(\mathbf{K})) = K$, and vice versa since $\mathcal{S}(\mathbf{K})$ is uniquely determined by \mathbf{K} . \square

According to (9) and *Proposition 1*, if \mathbf{R}_x is low-rank with $\text{Rank}(\mathbf{R}_x) \leq 2 \min\{N, M\} - 2$ and we can obtain the estimation of the low-rank \mathbf{K} as $\widetilde{\mathbf{K}}$ with a decomposition in the form of (14), then $\mathcal{S}(\widetilde{\mathbf{K}})$ is guaranteed to be the exact estimation of \mathbf{R}_x .

Next, considering the equivalence between (6a) and (6b), to implement the structure of \mathbf{K} as (14) in the solution, we relax $\text{Rank}(\mathbf{K})$ to its convex ℓ_1 -norm form $\sum_{i=1}^K r_i$, and then obtain the formulation

$$\begin{aligned} \{\widetilde{\mathbf{K}}, \widetilde{\mathbf{r}}, \widetilde{\mathbf{f}}_1, \widetilde{\mathbf{f}}_2\} &= \arg \min_{\mathbf{K}, \mathbf{r}, \mathbf{f}_1, \mathbf{f}_2} \sum_{i=1}^K r_i \\ \text{s.t.} \quad & \left\| \widehat{\mathbf{R}}_y - \mathcal{J}\mathcal{S}(\mathbf{K})\mathbf{J}^H \right\|_F^2 \leq \beta, \\ & \mathbf{K} = \mathbf{A}'_M(\mathbf{f}_2) \text{diag}(\mathbf{r}) \mathbf{A}'_N(\mathbf{f}_1)^T, \\ & \mathcal{S}(\mathbf{K}) \succeq 0. \end{aligned} \quad (15)$$

Noticeably, following the definition of the decoupled-based atomic norm [17, 18], a decoupled-based atomic norm of \mathbf{K} over the matrix-form atom set $\mathcal{A}'_d = \{\mathbf{a}'_M(f_2) \mathbf{a}'_N(f_1)^H \mid f_1, f_2 \in (-\frac{1}{2}, \frac{1}{2})\}$ can be expressed as

$$\|\mathbf{K}\|_{\mathcal{A}'_d} = \inf \left\{ \sum_{i=1}^K r_i \mid \mathbf{K} = \sum_{i=1}^K r_i \mathbf{a}'_M(f_{2,i}) \mathbf{a}'_N(f_{1,i})^T \right\}. \quad (16)$$

Accordingly, under the condition $K \leq 2 \min\{N, M\} - 2$, we rewrite (15) into the D-ANM form

$$\begin{aligned} \widetilde{\mathbf{K}} &= \arg \min_{\mathbf{K}} \|\mathbf{K}\|_{\mathcal{A}'_d} \\ \text{s.t.} \quad & \left\| \widehat{\mathbf{R}}_y - \mathcal{J}\mathcal{S}(\mathbf{K})\mathbf{J}^H \right\|_F^2 \leq \beta, \\ & \mathcal{S}(\mathbf{K}) \succeq 0. \end{aligned} \quad (17)$$

Finally, we obtain the enhanced-LRSCR via D-ANM (LRSCR-D-ANM), by reformulating (17) as its SDP formulation [17, 18]

$$\begin{aligned} \{\widetilde{\mathbf{K}}, \widetilde{\mathbf{u}}'_N, \widetilde{\mathbf{u}}'_M\} &= \arg \min_{\mathbf{K}, \mathbf{u}'_N, \mathbf{u}'_M} \frac{1}{2c} (\text{Tr}(\mathbf{T}(\mathbf{u}'_N)) + \text{Tr}(\mathbf{T}(\mathbf{u}'_M))) \\ \text{s.t.} \quad & \left\| \widehat{\mathbf{R}}_y - \mathcal{J}\mathcal{S}(\mathbf{K})\mathbf{J}^H \right\|_F^2 \leq \beta, \\ & \begin{bmatrix} \mathbf{T}(\mathbf{u}'_M) & \mathbf{K} \\ \mathbf{K}^H & \mathbf{T}(\mathbf{u}'_N) \end{bmatrix} \succeq 0, \\ & \mathcal{S}(\mathbf{K}) \succeq 0, \end{aligned} \quad (18)$$

where $\mathbf{u}'_N \in \mathbb{C}^{2N-1}$, $\mathbf{u}'_M \in \mathbb{C}^{2M-1}$, and $c = \sqrt{(2N-1)(2M-1)}$.

Remark 2: It is worth noting that the two-level Toeplitz matrix $\mathcal{S}(\widetilde{\mathbf{K}})$ constructed by the optimal solution $\widetilde{\mathbf{K}}$ from (18) is guaranteed to hold the generalized Vandermonde decomposition as long as $K \leq 2 \min\{N, M\} - 2$. Obviously, this condition is $2\times$ looser than the original one $K \leq \min\{N, M\} - 1$ required by the basic LRSCR in (8) which is however too conservative for the MMV case as discussed in *Remark 1*. Such a boost in the upper-bound on K is due to the enlarged sizes $2N-1$ and $2M-1$ of the 2D manifolds $\mathbf{a}'_N(f_{1,i})$ and $\mathbf{a}'_M(f_{2,i})$ in (13) through utilizing the structure of \mathbf{K} in (14), compared with the N -size $\mathbf{a}_N(f_{1,i})$ and M -size $\mathbf{a}_M(f_{2,i})$ in (2).

3.3. Harmonic Retrieval

Given $\widetilde{\mathbf{K}}$, $\mathbf{T}(\widetilde{\mathbf{u}}'_N)$ and $\mathbf{T}(\widetilde{\mathbf{u}}'_M)$ from (18), specific off-the-shelf spectral analysis tools can be employed for estimating the 2D frequencies \mathbf{f}_1 and \mathbf{f}_2 , such as, the matrix pencil and pairing (MaPP) based on $\mathcal{S}(\widetilde{\mathbf{K}})$ [10], the Vandermonde decomposition based harmonic retrieval and pairing based on $\mathbf{T}(\widetilde{\mathbf{u}}'_N)$ and $\mathbf{T}(\widetilde{\mathbf{u}}'_M)$ [17, 18], etc.

4. LOW-COMPLEXITY IMPLEMENTATION

According to [19], the computational complexity in solving LRSCR-D-ANM in (18) is $\mathcal{O}((NM)^{4.5})$ which is in the same order as that of the basic LRSCR in (8), due to their comparable problem scales dominated by the same largest-size PSD constraints, i.e., $\mathbf{T}_{2D}(\mathbf{u}_{R_x}, \mathbf{v}_{R_x}) \succeq 0$ in (8) and $\mathcal{S}(\mathbf{K}) \succeq 0$ in (18), respectively.

On the other hand, thanks to the strong structure of \mathbf{K} in (14) captured via the D-ANM as (16), the LRSCR-D-ANM in (18) can also be implemented without the third PSD constraint $\mathcal{S}(\mathbf{K}) \succeq 0$ (LRSCR-D-ANM-w/o3). Accordingly, with the remaining smaller-size PSD constraint $[\mathbf{T}(\mathbf{u}'_M), \mathbf{K}; \mathbf{K}^H, \mathbf{T}(\mathbf{u}'_N)] \succeq 0$, the complexity of the LRSCR-D-ANM-w/o3 drops down to $\mathcal{O}((NM)^2(N+M)^{2.5})$, which is 2.5 orders lower than that of the LRSCR-D-ANM when $N = M$. In this sense, the LRSCR-D-ANM-w/o3 actually enables a tradeoff option to balance the performance and the complexity of 2D harmonic retrieval, which is unavailable to the basic LRSCR.

5. SIMULATIONS

This section presents numerical results to evaluate the performance and the complexity of the LRSCR-D-ANM solutions, while the basic LRSCR is considered as benchmark. For a fair comparison, all methods use an off-the-shelf SDP-based solver [20], and incorporate the MaPP as mentioned in Subsection 3.3 for obtaining the 2D frequencies [10]. All simulations run on a computer with a 4-core Intel i7-6500U 2.50GHz CPU and 8GB memory. The root mean squared error (RMSE) is measured to evaluate

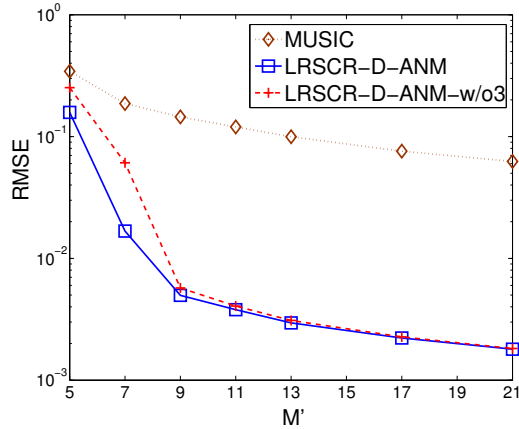


Fig. 1. RMSE vs. M' : MUSIC, LRSCR-D-ANM and LRSCR-D-ANM-w/o3, when $N=M=5$, $L=200$, $K=3$ and $\text{SNR}=5\text{dB}$.

the estimation accuracy of 2D harmonic retrieval as $\text{RMSE} = \frac{1}{K} \sum_{i=1}^K \left(\frac{1}{M_t} \sum_{n=1}^{M_t} \left((\tilde{f}_{1,i}^n - f_{1,i})^2 + (\tilde{f}_{2,i}^n - f_{2,i})^2 \right) \right)^{\frac{1}{2}}$, where M_t , $\tilde{f}_{1,i}^n$ and $\tilde{f}_{2,i}^n$ denote the number of Monte-Carlo trials, and the estimates of $f_{1,i}$ and $f_{2,i}$ in the n -th trial, respectively. In each trial, for K uncorrelated sources, their frequencies are generated under a sufficient frequency separation condition, i.e., $\Delta_{\min} \triangleq \min \max_{i \neq j} \{|f_{1,i} - f_{1,j}|, |f_{2,i} - f_{2,j}|\} \geq \frac{1.19}{\min\{N, M\}}$ [21], and observed through a compressive random Gaussian matrix \mathbf{J} as (3) with the compression ratio $\frac{M'}{NM}$ [22], at $\text{SNR} = 10 \log_{10} \left(\frac{\sigma_r}{\sigma^2} \right)$ with $r_i = r \forall i$ for simplicity.

5.1. Influence of the Third PSD Constraint

First, we evaluate the influence of the third PSD constraint in (18) on the performance of the proposed LRSCR-D-ANM. Fig. 1 shows that the LRSCR-D-ANM with the third PSD constraint slightly outperforms the one without this constraint (LRSCR-D-ANM-w/o3), which indicates the role of the PSD property of the covariance in enhancing the estimation performance. However, as can be observed the performance gap diminishes as M' goes large. Similar results have also been observed as SNR and L increases. Considering that the removal of the third PSD constraint can reduce the computational complexity as has been discussed in Section 4, the LRSCR-D-ANM-w/o3 is an efficient alternative to the LRSCR-D-ANM with a negligible loss in accuracy, for example when $M' \geq 13$ in Fig. 1. Meanwhile, the performance of the classic subspace method is also tested in Fig. 1, where the LRSCR-D-ANM always outperforms MUSIC [23].

5.2. Condition on the Number of 2D Harmonics

Next, we test different methods using a varying number of 2D harmonics. For the basic LRSCR, when the conservative condition on K does not hold, i.e., $K > \min\{N, M\} - 1$, an extra checking mechanism is used as proposed in [10]. In Fig. 2, the performance of the basic LRSCR degrades dramatically after K becomes larger than 4. This is because the checking mechanism mostly outputs the "false" status, which indicates it judges that the generalized Vandermonde decomposition does not exist. On the other hand, the proposed LRSCR-D-ANM and LRSCR-D-ANM-w/o3 both work properly without using any extra checking mechanism as long as $K \leq 2 \min\{N, M\} - 2$.

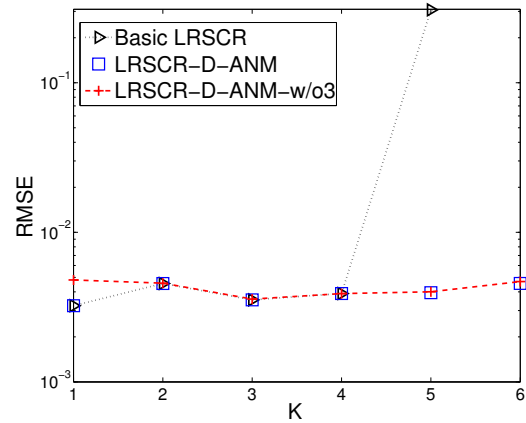


Fig. 2. RMSE vs. K : basic LRSCR, LRSCR-D-ANM and LRSCR-D-ANM-w/o3, when $N=M=5$, $M'=15$, $L=200$ and $\text{SNR}=5\text{dB}$.

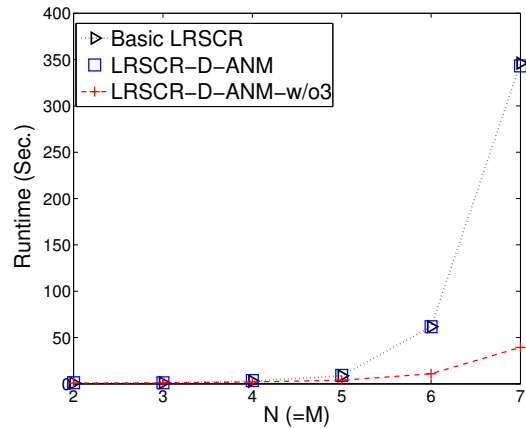


Fig. 3. Runtime vs. $N(=M)$: basic LRSCR, LRSCR-D-ANM and LRSCR-D-ANM-w/o3, when $M' = \lfloor \frac{NM}{2} \rfloor + 1$, and $L=200$.

5.3. Computational Complexity

The computational complexity in terms of runtime are measured and compared among different methods. As shown in Fig. 3, the LRSCR-D-ANM-w/o3 runs (much) faster than the basic LRSCR and the LRSCR-D-ANM especially when N and M grow large, thanks to the reduced problem scale after removing the largest-size PSD constraint. Combining this complexity result with the estimation performance from Fig. 1 and Fig. 2, the LRSCR-D-ANM-w/o3 works as an excellent option to balance the estimation accuracy and the computational costs for practical implementations.

6. CONCLUSION

Given the sample covariance, an efficient 2D harmonic retrieval technique is developed under the LRSCR framework. The strong structure of the kernel matrix hidden in the covariance is well captured by transferring the basic LRSCR based on the covariance to an enhanced LRSCR based on its kernel matrix, through D-ANM over a matrix-form atom set defined according to the enlarged manifolds. This thus enables the LRSCR-D-ANM to retrieve more detectable 2D harmonics than the basic LRSCR. Further, a low-complexity solution of the LRSCR-D-ANM is proposed to achieve a nice tradeoff between the performance and complexity in 2D harmonic retrieval.

7. REFERENCES

- [1] G. Tang, B. N. Bhaskar, P. Shah, and B. Recht, "Compressed sensing off the grid," *IEEE Transactions on Information Theory*, vol. 59, no. 11, pp. 7465–7490, Nov. 2013.
- [2] B. N. Bhaskar, G. Tang, and B. Recht, "Atomic norm denoising with applications to line spectral estimation," *IEEE Transactions on Signal Processing*, vol. 61, no. 23, pp. 5987–5999, Dec. 2013.
- [3] Y. Li and Y. Chi, "Off-the-grid line spectrum denoising and estimation with multiple measurement vectors," *IEEE Transactions on Signal Processing*, vol. 64, no. 5, pp. 1257–1269, Mar. 2016.
- [4] X. Wu, W. Zhu, and J. Yan, "A Toeplitz covariance matrix reconstruction approach for direction-of-arrival estimation," *IEEE Transactions on Vehicular Technology*, vol. 66, no. 9, pp. 8223–8237, Sept. 2017.
- [5] Y. Wang, Y. Zhang, Z. Tian, G. Leus, and G. Zhang, "Super-resolution channel estimation for arbitrary arrays in hybrid millimeter-wave massive MIMO systems," *IEEE Journal of Selected Topics in Signal Processing*, vol. 13, no. 5, pp. 947–960, Sept. 2019.
- [6] P. Pal and P. P. Vaidyanathan, "A grid-less approach to under-determined direction of arrival estimation via low rank matrix denoising," *IEEE Signal Processing Letters*, vol. 21, no. 6, pp. 737–741, June 2014.
- [7] Hongbin Li, P. Stoica, and Jian Li, "Computationally efficient maximum likelihood estimation of structured covariance matrices," *IEEE Transactions on Signal Processing*, vol. 47, no. 5, pp. 1314–1323, May 1999.
- [8] X. Tian, J. Lei, and L. Du, "A generalized 2-D DOA estimation method based on low-rank matrix reconstruction," *IEEE Access*, vol. 6, pp. 17 407–17 414, 2018.
- [9] W. Xu, J. Cai, K. V. Mishra, M. Cho, and A. Kruger, "Precise semidefinite programming formulation of atomic norm minimization for recovering d -dimensional ($d \geq 2$) off-the-grid frequencies," in *Proc. Information Theory and Applications Workshop (ITA)*, Feb. 2014, pp. 1–4.
- [10] Z. Yang, L. Xie, and P. Stoica, "Vandermonde decomposition of multilevel Toeplitz matrices with application to multidimensional super-resolution," *IEEE Transactions on Information Theory*, vol. 62, no. 6, pp. 3685–3701, June 2016.
- [11] Y. Wang, Z. Tian, S. Feng, and P. Zhang, "Efficient channel statistics estimation for millimeter-wave MIMO systems," in *Proc. IEEE Int. Conf. Acoustics Speech and Signal Processing (ICASSP)*, Mar. 2016, pp. 3411–3415.
- [12] —, "A fast channel estimation approach for millimeter-wave massive MIMO systems," in *Proc. IEEE Global Conf. Signal and Information Processing (GlobalSIP)*, Dec. 2016, pp. 1413–1417.
- [13] Y. Wang, P. Xu, and Z. Tian, "Efficient channel estimation for massive MIMO systems via truncated two-dimensional atomic norm minimization," in *Proc. IEEE Int. Conf. Communications (ICC)*, May 2017, pp. 1–6.
- [14] Z. Liu, Z. Huang, and Y. Zhou, "Array signal processing via sparsity-inducing representation of the array covariance matrix," *IEEE Transactions on Aerospace and Electronic Systems*, vol. 49, no. 3, pp. 1710–1724, July 2013.
- [15] B. Ottersten, P. Stoica, and R. Roy, "Covariance matching estimation techniques for array signal processing applications," *Digital Signal Processing*, vol. 8, pp. 185–210, 1998.
- [16] Y. Zhang, G. Zhang, and X. Wang, "Computationally efficient doa estimation for monostatic mimo radar based on covariance matrix reconstruction," *Electronics Letters*, vol. 53, no. 2, pp. 111–113, 2016.
- [17] Z. Tian, Z. Zhang, and Y. Wang, "Low-complexity optimization for two-dimensional direction-of-arrival estimation via decoupled atomic norm minimization," in *Proc. IEEE Int. Conf. Acoustics Speech and Signal Processing (ICASSP)*, Mar. 2017, pp. 3071–3075.
- [18] Z. Zhang, Y. Wang, and Z. Tian, "Efficient two-dimensional line spectrum estimation based on decoupled atomic norm minimization," *Signal Processing*, vol. 163, pp. 95–106, Oct. 2019.
- [19] L. Vandenberghe and S. Boyd, "Semidefinite programming," *SIAM review*, vol. 38, no. 1, pp. 49–95, 1996.
- [20] M. Grant and S. Boyd, "CVX: Matlab software for disciplined convex programming, version 2.1," <http://cvxr.com/cvx>, Mar. 2014.
- [21] Y. Chi and Y. Chen, "Compressive two-dimensional harmonic retrieval via atomic norm minimization," *IEEE Transactions on Signal Processing*, vol. 63, no. 4, pp. 1030–1042, Feb. 2015.
- [22] S. Li, D. Yang, G. Tang, and M. B. Wakin, "Atomic norm minimization for modal analysis from random and compressed samples," *IEEE Transactions on Signal Processing*, vol. 66, no. 7, pp. 1817–1831, Apr. 2018.
- [23] R. Schmidt, "Multiple emitter location and signal parameter estimation," *IEEE Transactions on Antennas and Propagation*, vol. 34, no. 3, pp. 276–280, Mar. 1986.